arXiv:1610.03119v2 [cond-mat.quant-gas] 31 Oct 2016

Superfluid filaments of dipolar bosons in free space

Fabio Cinti,[1,2,*] Alberto Cappellaro,[3,†] Luca Salasnich,[3,4,‡] and Tommaso Macrì[5,§]

[1] *National Institute for Theoretical Physics (NITheP), Stellenbosch 7600, South Africa*
[2] *Institute of Theoretical Physics, Stellenbosch University, Stellenbosch 7600, South Africa*
[3] *Dipartimento di Fisica e Astronomia Galileo Galilei and CNISM, Università di Padova, via Marzolo 8, 35131 Padova, Italy*
[4] *CNR-INO, via Nello Carrara, 1 - 50019 Sesto Fiorentino, Italy*
[5] *Departamento de Física Teórica e Experimental, Universidade Federal do Rio Grande do Norte, and International Institute of Physics, Natal-RN, Brazil*

(Dated: November 1, 2016)

We systematically investigate the zero temperature phase diagram of bosons interacting via dipolar interactions in three dimensions in free space via path integral Monte Carlo simulations based on the worm algorithm. Upon increasing the strength of the dipolar interaction and at sufficiently high densities we find a wide region where filaments are stabilized along the direction of the external field. Most interestingly by computing the superfluid fraction we conclude that superfluidity is anisotropic and vanishes along the orthogonal plane. Finally we perform simulations at finite temperature confirming the stability of filaments against thermal fluctuations and provide an estimate of the superfluid fraction in the weak coupling limit in the framework of the Landau two-fluid model. Such findings suggest that in the thermodynamic limit the system might crystallize into a regular array of superfluid filaments which are not globally phase coherent.

PACS numbers: 05.30.-d, 03.75.Hh, 03.75.Kk, 03.75.Nt, 67.85.De, 67.85.Bc, 67.80.K-

Superfluidity is an amazing phenomenon of quantum mechanical origin that manifests macroscopically as frictionless flow and lack of response to rotation for small enough angular velocity [1]. The two-fluid model is an effective theory of superfluids, where the system is thought as made up of two fluids, one which behaves as an ideal fluid, and the other as an ordinary liquid. This phenomenological description may be obtained from the microscopic concept of a superfluid as being constituted of a Bose-Einstein condensate and its elementary excitations. The Landau criterion establishes the existence of a critical velocity, based on the shape of the excitation spectrum, above which the system loses its superfluid features [2].

Several experimental platforms have been used to investigate quantum matter in the superfluid regime [3]. Among them, ultracold gases realize a very clean and controllable many-body playground that permit the observation of quantum properties with unprecedented precision [4]. In these systems superfluidity has been observed both with bosonic as well as with fermionic atoms [5–8]. The superfluid fraction, the ratio of the superfluid density to the total density of the system, has been recently measured in two-component Fermi gas interacting via strong contact potentials [7, 9, 10]. An even richer phenomenology appears when long-range interactions are present. The non-local character of the interparticle potential may induce instabilities of the density that lead to a spontaneous breaking of translational symmetry. A primary example is the long sought supersolid state, where superfluidity is accompanied by a crystalline order [11–13]. Recent groundbreaking experiments with dipolar condensates demonstrated the existence of dense bosonic droplets in trapped configurations [14–17] and in free space [18]. Beyond mean-field effects [19–21] and three-body interactions [22] have been invoked as the main mechanisms responsible for the stability of these clusters. Large scale simulations based on a non-local non-linear Schrödinger equation have shown very good agreement with the density distribution and the excitation spectra observed in laboratory. Latest experiments paved the way for the search of phase coherence of droplets, demonstrating interference pattern via expansion dynamics of the condensate. The presence of fringes showed that each droplet individually is phase coherent and thus superfluid, leaving yet unresolved the question of global phase coherence of the system [15].

In this Letter we report path-integral Monte Carlo (PIMC) results for the low temperature properties of a dipolar gas of bosons in three dimensional free space. Recent works showed with similar methods the existence of a window in parameter space leading to stable self-bound configurations of a single [23] or several droplets in a regular arrangement in trapped configurations [24]. Yet no work has investigated the superfluid character of these structures until now. Here we address the issue of superfluidity of elongated filaments for a wide range of the strength of the dipolar interaction and density as well as their stability against finite temperature fluctuations. We carry out large scale simulations, based on a continuous-space worm algorithm (WA) which allows for an efficient and reliable determination of the superfluid density [25, 26]. We observe an anisotropic character of the superfluid fraction in the inhomogeneous regime of the filaments. Most importantly, we predict the absence of global phase coherence and therefore exclude

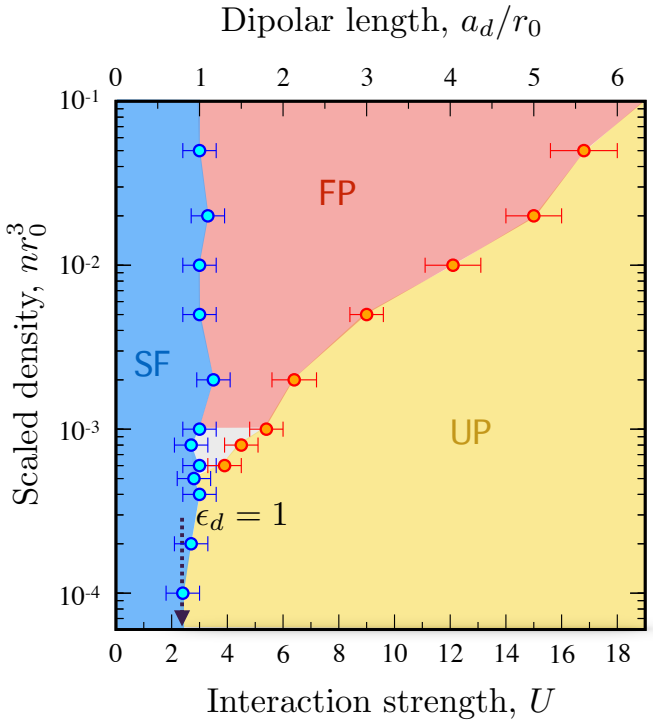

FIG. 1. Zero-temperature phase diagram of dipolar bosons in three dimensions in free space. The phase diagram displays the emergence of superfluid (SF), and superfluid filaments (FP) and unstable non-superfluid cluster phases (UP) for varying dimensionless interaction strength U (or equivalently dipolar length a_d/r_0) and scaled density nr_0^3. For $a_d/r_0 \lesssim 0.9$ the blue region labeled by SF corresponds to a uniform superfluid. For low densities the SF regime agrees with mean-field prediction that predicts stability for $a_d/a_s < 1$ (black dotted arrow at $a_d/r_0 = 0.75$). Superfluid filament phase (FP) is encountered for high densities $nr_0^3 \gtrsim 5 \cdot 10^{-4}$ and for dipolar lengths $a_d/r_0 \gtrsim 1$ and extends to strong couplings. In contrast, for small densities $nr_0^3 \lesssim 5 \cdot 10^{-4}$ or very strong interactions the system collapses into tiny clusters with vanishing superfluid fraction, see also Fig.2c. The phase boundaries in the dashed region are not resolved.

the existence of supersolidity in three dimensional dipolar bosons. The Hamiltonian of an ensemble of N interacting identical bosons is:

$$\hat{H} = -\sum_{i=1}^{N} \frac{\hbar^2}{2m}\nabla_i^2 + \sum_{i<j}^{N} V(\mathbf{r}_i - \mathbf{r}_j), \qquad (1)$$

where m is the particle mass, $\mathbf{r}_i$ is the position of the i-th dipole. We model the interparticle potential $V(\mathbf{r})$ by a short-range hard-core with cutoff r_0 and an anisotropic long-range dipolar potential:

$$V(\mathbf{r}) = \begin{cases} \frac{C_{dd}}{4\pi}\frac{1-3\cos^2\theta}{r^3} & \text{if } r \geq r_0, \\ \infty & \text{if } r < r_0, \end{cases} \qquad (2)$$

where $C_{dd}/4\pi$ is the coupling constant and the angle θ denotes the angle between the vector $\mathbf{r}$ and the z-axis. Here the units of length and energy are r_0 and $\hbar^2/mr_0^2$, respectively. Therefore the zero-temperature physics is controlled by the dimensionless interaction strength $U = mr_0^2 C_{dd}/4\pi\hbar^2$ and the dimensionless density nr_0^3 only [27]. The Hamiltonian Eq.(1) applies both to vertically aligned dipoles interacting via magnetic or electric dipole moments. For magnetic dipoles $C_{dd} = \mu_0\mu_d^2$ with μ_0 the vacuum permeability and μ_d the magnetic moment of the atom, for electric dipoles $C_{dd} = d^2/\epsilon_0$ with ϵ_0 the permittivity of the vacuum and d the dipole moment [28]. The presence of the hard-core potential with radius r_0 removes the unphysical $1/r^3$ attractive interaction of two aligned dipoles in head-to-tail configurations at small distances. For vanishing dipolar interactions the hard-core sets the value of the scattering length a_s associated to Eq.(2) to $a_s = r_0$. Finite dipolar potentials modify a_s which turns out to be a non trivial function of the coupling constant strength $a_s = a_s(C_{dd})$ [29, 30]. This observation turns out to be crucial to account for the proper stability diagram of a dipolar gas in generic mean-field (and beyond mean-field) approaches. For example a standard Bogoliubov calculation determines the stability of a dilute homogeneous condensate when the inequality $\epsilon_d \equiv a_d/a_s < 1$ is satisfied, where $a_d = \frac{C_{dd}m}{12\pi\hbar^2}$ is the dipolar length associated to the dipolar potential [28, 31].

In order to assess systematically the zero temperature phases, we determine the equilibrium properties of Eq. (1) in a wide range of scaled density nr_0^3 and interaction strength U. We work in the canonical ensemble, i.e. fixing the particle number, chosen between $N = 100 - 400$ in a cubic box with linear dimension L with periodic boundary conditions. From these simulations we obtain, for example, density profiles, and pair correlation functions, as well as the superfluid fraction [32] at finite temperatures. The phases of the system were obtained by extrapolating to the limit of zero temperature, starting from temperatures of the order of the superfluid-normal transition temperature T_0 of an ideal Bose gas with the same density [1], and then lowering the temperature until observables, such as the total energy, superfluid fraction and pair correlations did not change on further decrease of T. The observables such as the superfluid fraction, the density profile and pair correlation function were then analyzed to construct the phase diagram in Fig.1 that we now discuss in detail. For clarity an additional horizontal axis displays the scaled dipolar length a_d/r_0. In the weakly interacting regime the system is in a superfluid phase (SF) with unitary f_s. For low densities $n\, r_0^3 \lesssim 10^{-3}$ the SF extends up to $U \approx 2.25$ which agrees with the mean-field phase boundary predicted by standard Bogoliubov analysis ($\epsilon_d = 1$) for the dipolar potential and a contact interaction. Increasing the interaction strength the system enters into an unstable phase (UP) with vanishing superfluidity and characterized by droplet structures with few particles. For higher densi-

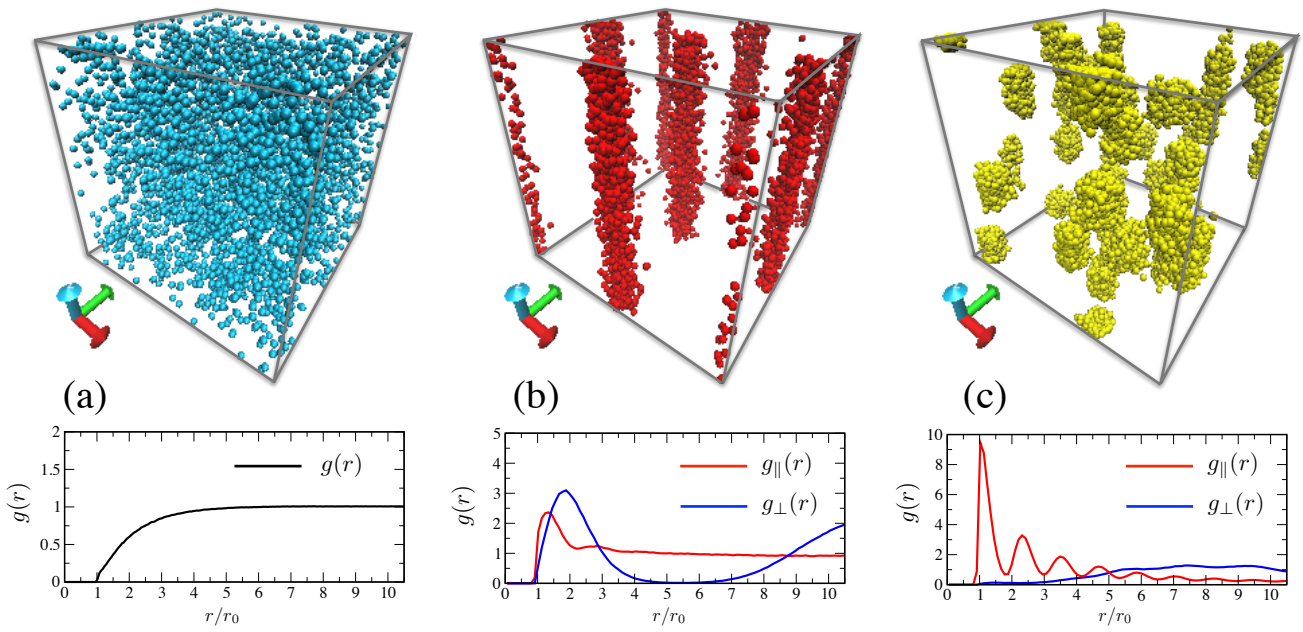

FIG. 2. Characterization of the different phases across the phase diagram at large density. Upper panels. PIMC shapshots at different strengths of dipolar interaction for $nr_0^3 = 10^{-2}$ in the three phases: (a) SF phase at $a_d = 0.6r_0$, (b) superfluid FP phase at $a_d = 2.6r_0$ and (c) UP at $a_d = 6.0r_0$. Lower panels. (a) pair correlation functions $g(r)$ in the superfluid phase. (b) and (c) pair correlation functions $g_\parallel(r)$ along the vertical direction (red) and $g_\perp(r)$ along the orthogonal plane (blue). $g_\parallel(r)$ has a fluid-like profile in the FP phase. In the UP $g_\parallel(r)$ a high peak due to strong attractive interactions appears at distances $r \gtrsim r_0$. $g_\perp(r)$ in the FP phase shows a strong suppression in between two filaments whereas in the UP it flattens rapidly at intermediate distances. Simulations for this figure are done with 100 particles and 500 slices with periodic boundary conditions in free space. Correlation functions are averaged over a hundred configurations.

ties $nr_0^3 > 6 \cdot 10^{-4}$, crossing the SF phase boundary, the system goes into an extended cluster phase characterized by elongated filaments (FP) with anisotropic superfluid fraction (see below). We notice that this FP extends from small positive induced contact potential ($\epsilon_d \gtrsim 1$) which corresponds to the experimentally relevant regime of [14], to the strongly coupled limit of large dipolar interactions and large densities. For intermediate densities $6 \cdot 10^{-4} \lesssim nr_0^3 \lesssim 1 \cdot 10^{-3}$ the phase boundaries are not completely resolved (grey region in Fig.1).

Snapshots of representative configurations with 100 particles and 500 imaginary-time slices ($n\,r_0^3 = 10^{-2}$) are shown in Fig.2. In the SF phase (Fig.2a) particles delocalize into a uniform gas and display a flat pair correlation function, $g(r)$, typical of a fluid phase of particles interacting via hard-core two-body potential. In Fig.2b a typical configuration of the FP is illustrated where filaments elongate along the vertical direction. Finally in the UP several small clusters form, slightly elongated along the vertical direction, signaling a fragmentation of the filaments for large interactions. In the non-homogeneous FP and UP phases we analyze the pair correlation function $g(r)$ along two orthogonal directions. The function $g_\parallel(r)$ (red line in Fig.2) is computed along the vertical axis parallel to the direction of the filaments. In the FP phase $g_\parallel(r)$ has a liquid-like profile with a peak $r \gtrsim r_0$ as a consequence of the attractive part of the dipolar interaction and the large density along the z-axis. In the UP the first peak of $g_\parallel(r)$ is higher and the function oscillates several times before vanishing for large distances as a consequence of the finite size of the clusters. The correlation $g_\perp(r)$ (blue line in Fig.2) is evaluated along the horizontal plane, perpendicular to the direction of the filaments. In the FP phase, it is strongly suppressed in the region between two filaments as expected from the configuration snapshot. From the distance of the second peak we also estimate an average distance between the filaments $d \approx 10\,r_0$. In the UP $g_\perp(r)$ flattens at intermediate distances displaying an irregular arrangement of the small dipolar droplets along the horizontal plane.

To fully characterize the genuine quantum properties of the FP we compute the superfluid fraction $f_s^{(i)}$ as a function of the interaction strength and temperature along three orthogonal directions $i = x, y, z$, yielding:

$$f_s^{(i)} = \frac{m}{\hbar^2 \beta\, n} \langle w_i^2 \rangle, \tag{3}$$

where $\beta{=}1/(k_B T)$ with k_B the Boltzmann constant, being w_i the winding number estimator, and $\langle \ldots \rangle$ stands for its thermal average [33]. By definition w_i reports the number of times the particle paths wind around the periodic cell [34]. Fig.3 depicts the superfluid fraction $f_s^{(i)}$

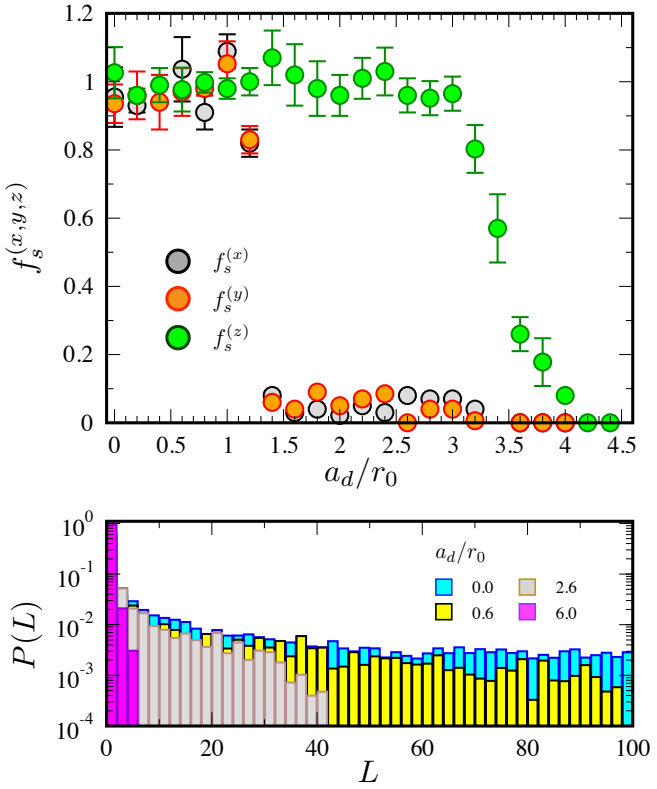

FIG. 3. Superfluid fraction across the transition from superfluid to filament transition at high densities. Upper panel. Superfluid fraction as a function of the dipolar length along the vertical direction and the orthogonal direction for $nr_0^3 = 10^{-2}$. Dipoles and filaments are aligned along the z-axis. In the SF phase the superfluid fraction converges to $f_s = 1$ isotropically. In the filaments we observe $f_s = 1$ along the vertical axis and vanishing on the orthogonal plane which implies that the system is not expected to be globally phase-coherent. Error bars are statistical uncertainties. When the error bar is not shown, then it is smaller than the symbol size. Lower panel. Relative frequency of permutation cycles of length L again for $nr_0^3 = 10^{-2}$ and $a_d = 0, 0.6, 2.8, 6.0\, r_0$ in the the SP phase (light blue and yellow), FP phase (grey) and UP (purple).

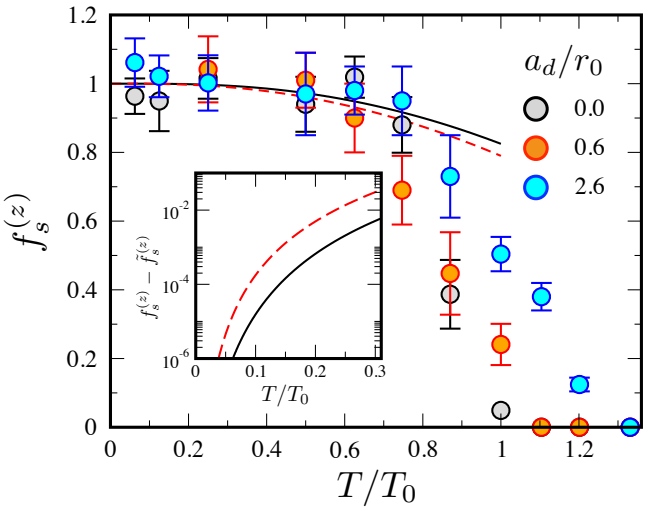

FIG. 4. Superfluid fraction at finite temperature. Plot of the superfluid fraction $f_s^{(z)}$ as a function of the temperature T scaled by the critical temperature of the non-interacting Bose gas T_0 at $nr_0^3 = 10^{-2}$ for three values of the dipolar lengths: a) SF with $a_d = 0$ (short-range hard-core bosons), b) SF with $a_d = 0.6 r_0$, c) FP with $a_d = 2.6 r_0$. Error bars are statistical uncertainties. When the error bar is not shown, it is smaller than the symbol size. Lines refer to the analytical prediction of the temperature dependence of the superfluid fraction at $nr_0^3 = 10^{-2}$ from Eq.(4) in the framework of two-fluid Landau theory in the SF at $a_d = 0$ (black continuous line) and $a_d = 0.6\, r_0$ (red dashed line). Inset. Low temperature limit of the superfluid fraction from Eq.(4) and Eq.(6) in the SF at $a_d = 0$ (black continuous line) and $a_d = 0.6\, r_0$ (red dashed line).

calculated varying the dipolar length a_d for $nr_0^3 = 10^{-2}$. In the SF phase the superfluid density is uniform and unitary ($f_s^{(i)} = 1$). Crossing the SF-FP phase boundary $f_s^{(i)}$ displays a strong anisotropy. The superfluid fraction is unitary along the vertical direction and it vanishes along the orthogonal $x-y$ plane, showing only a marginal finite-size effect contribution to w_x and w_y, respectively. This result indicates that each filament is phase coherent, but globally the system is not. Finally entering in the UP $f_s^{(i)} = 0$ uniformly as expected from the fragmentation of the filaments in the configurations. The lower panel of Fig.3 reports the relative frequency of exchange cycles involving a particle number $1 \leq L \leq N$ [35], for the set of parameters $a_d = 0, 0.6, 2.6, 6.0\, r_0$. In the SF phase we observe permutation cycles which are as long as the particle number N. In the FP cycles reduce to few tens of particles in support of the previous observation that superfluidity originates within each filament. Lastly, in the UP, only few bosons take part in permutation cycles, indicating that they can exchange at most within each cluster containing few atoms.

Finally we investigate the stability of superfluid filaments at finite temperature T. In Fig.4 we show the temperature dependent superfluid fraction for a system of $N = 100$ particles at density $nr_0^3 = 10^{-2}$ scaled by the critical temperature of an ideal Bose gas with the same density $k_B T_0 = \frac{2\pi}{\zeta(3/2)^{2/3}} \left(nr_0^3\right)^{2/3}$ [36]. Our results indeed show that for a large range of temperatures we observe finite superfluidity as well as stability of the filaments. We start by analyzing the superfluid fraction in the SF at $nr_0^3 = 10^{-2}$. We compare PIMC results with an analytical calculation within the Landau two-fluid model [2], which, for an uniform system, predicts the temperature dependence of the superfluid fraction as

$$f_s^{(z)} = 1 + \frac{1}{3n} \int \frac{d^3q}{(2\pi)^3} \frac{\hbar^2 q^2}{m} \frac{df_B}{dE_{\mathbf{q}}} \qquad (4)$$

where $f_B = (e^{\beta E_{\mathbf{q}}} - 1)^{-1}$ is the Bose distribu-

tion function, and $E_{\mathbf{q}} = \sqrt{\frac{\hbar^2 q^2}{2m}\left(\frac{\hbar^2 q^2}{2m} + 2\mu\tilde{V}_{\rm ps}(\mathbf{q})\right)}$ the Bogoliubov spectrum. The function $\tilde{V}_{\rm ps}(\mathbf{q}) = g_0\left(1-\epsilon_d+3\epsilon_d\cos^2(\theta_q)\right)$ is the Fourier transform of the pseudo-potential $V_{\rm ps}(\mathbf{r}) = g_0\delta(\mathbf{r}) + \frac{C_{dd}}{4\pi}\frac{1-3\cos^2\theta}{r^3}$ with $g_0{=}4\pi\hbar^2 a_s/m$, which is widely used as a regularized form of the interparticle potential (2) [28, 31, 37]. The chemical potential μ is estimated including the beyond mean field contribution of the dipolar interaction:

$$\mu = g_0 n\left(1+\frac{32}{3\sqrt{\pi}}\sqrt{n a_s^3}\,Q_{5/2}(\epsilon_d)\right), \qquad (5)$$

where $Q_\alpha(x){=}\int_0^1 dt\,\left(1-x+3xt^2\right)^\alpha$ [38]. The plot of $f_s^{(z)}$ from Eq.(4) is shown in Fig.4 for $a_d = 0$ (black line) and $a_d = 0.6\,r_0$ (red dashed line). In the low temperature regime we can linearize $E_{\mathbf{q}}$ to determine an approximate analytical formula for $f_s^{(z)}$:

$$\tilde{f}_s^{(z)} = 1 - \frac{2\pi^2}{45}Q_{-5/2}(\epsilon_d)\left(\frac{m}{\hbar^2}\right)^{3/2}\frac{(k_B T)^4}{n\,\mu^{5/2}}, \qquad (6)$$

that works well up to $T \lesssim 0.3\,T_0$. In the inset of Fig.4 we show the difference between the superfluid fractions of Eq.(4) and the analytical result Eq.(6) for the same values of a_d as in the main figure. For larger dipolar length $a_d = 2.6\,r_0$, in the FP, the superfluid fraction along the vertical axis is finite within a large window of temperatures. We conclude then that filaments are stable against finite temperature fluctuations and we clearly see that anisotropic superfluidity is finite up to temperature of the order of $0.8\,T_0$. We also verified that the orthogonal components $f_s^{(x,y)}$ are vanishing in this regime.

Our results suggest that the observed interference pattern [14] is a consequence of *local* phase coherence (within each filament) and not a *global* one (among the filaments). As we discussed above the FP is characterized by an anisotropic superfluid density that, interestingly, might be measured via the second sound along the orthogonal directions as recently done with strongly interacting Fermi gases [5–8].

In this Letter we studied the many-body phases of an ensemble of bosons interacting via dipole-dipole interactions in three dimensional free space and investigated the superfluid behavior of dipolar filaments. We spanned a wide range of the parameter space confirming the existence of an extended phase of non-overlapping filaments with unitary superfluidity along the filaments and vanishing otherwise. Our results therefore theoretically support recent experimental findings about the stability of droplets in free space [18] and the presence of local phase coherence [14] giving rise to interference fringes but exclude global phase coherence of the filaments and therefore a possible supersolid phase in the thermodynamic limit. Finally we confirmed that such a filament phase is stable at finite temperature. More refined investigations are needed to determine accurately the melting transition of the filaments into a fluid phase.

Acknowledgments. We thank S. Giorgini, G. Gori, T. Pohl, R. N. Bisset, M. Boninsegni, G. Shlyapnikov, F. Toigo and M. Troyer for useful discussions and I. Ferrier-Barbut for helpful correspondence. T.M. acknowledges CNPq for support through the fellowship Bolsa de produtividade em Pesquisa n. 311079/2015-6 and thanks NITheP for the hospitality where part of the work was done. F.C. gratefully acknowledges the hospitality of the Max Planck Institute for the Physics of Complex Systems, where part of the was carried out.

* cinti@sun.ac.za
† cappellaro@pd.infn.it
‡ luca.salasnich@unipd.it
§ macri@fisica.ufrn.br

[1] L. Pitaevskii and S. Stringari, *Bose-Einstein Condensation* (Oxford University Press, USA, 2003).
[2] C. Pethick and H. Smith, *Bose-Einstein condensation in dilute gases* (Cambridge University Press, Cambridge, England, 2002).
[3] A. J. Leggett, *Quantum liquids Bose condensation and Cooper pairing in condensed-matter systems* (Oxford University Press, 2006).
[4] I. Bloch, J. Dalibard, and W. Zwerger, Rev. Mod. Phys. **80**, 885 (2008).
[5] L. Verney, L. Pitaevskii, and S. Stringari, EPL (Europhysics Letters) **111**, 40005 (2015).
[6] M. K. Tey, L. A. Sidorenkov, E. R. S. Guajardo, R. Grimm, M. J. H. Ku, M. W. Zwierlein, Y.-H. Hou, L. Pitaevskii, and S. Stringari, Phys. Rev. Lett. **110**, 055303 (2013).
[7] L. P. Pitaevskii and S. Stringari, (2015), arXiv:1510.01306.
[8] Y.-H. Hou, L. P. Pitaevskii, and S. Stringari, Phys. Rev. A **88**, 043630 (2013).
[9] L. Salasnich, Phys. Rev. A **82**, 063619 (2010).
[10] L. A. Sidorenkov, M. K. Tey, R. Grimm, Y.-H. Hou, L. Pitaevskii, and S. Stringari, Nature **498**, 78 (2013).
[11] M. Boninsegni and N. V. Prokof'ev, Rev. Mod. Phys. **84**, 759 (2012).
[12] F. Cinti, T. Macrì, W. Lechner, G. Pupillo, and T. Pohl, Nature Communications **5**, 3235 EP (2014).
[13] J. Léonard, A. Morales, P. Zupancic, T. Esslinger, and T. Donner, (2016), arXiv:1609.09053.
[14] H. Kadau, M. Schmitt, M. Wenzel, C. Wink, T. Maier, I. Ferrier-Barbut, and T. Pfau, Nature **530**, 194 (2016).
[15] I. Ferrier-Barbut, H. Kadau, M. Schmitt, M. Wenzel, and T. Pfau, Phys. Rev. Lett. **116**, 215301 (2016).
[16] L. Chomaz, S. Baier, D. Petter, M. J. Mark, F. Wächtler, L. Santos, and F. Ferlaino, (2016), arXiv:1607.06613.
[17] I. Ferrier-Barbut, M. Schmitt, M. Wenzel, H. Kadau, and T. Pfau, (2016), arXiv:1609.03937.
[18] M. Schmitt, M. Wenzel, F. Böttcher, I. Ferrier-Barbut, and T. Pfau, (2016), 1607.07355.
[19] F. Wächtler and L. Santos, Phys. Rev. A **93**, 061603 (2016).
[20] R. N. Bisset, R. M. Wilson, D. Baillie, and P. B. Blakie,

Phys. Rev. A **94**, 033619 (2016).
[21] D. Baillie, R. M. Wilson, R. N. Bisset, and P. B. Blakie, Phys. Rev. A **94**, 021602 (2016).
[22] R. N. Bisset and P. B. Blakie, Phys. Rev. A **92**, 061603 (2015).
[23] H. Saito, Journal of the Physical Society of Japan **85**, 053001 (2016).
[24] A. Macia, J. Sánchez-Baena, J. Boronat, and F. Mazzanti, (2016), arXiv:1607.07184.
[25] M. Boninsegni, N. Prokof'ev, and B. Svistunov, Phys. Rev. Lett. **96**, 070601 (2006).
[26] M. Boninsegni, N. V. Prokof'ev, and B. V. Svistunov, Phys. Rev. E **74**, 036701 (2006).
[27] The scaled density nr_0^3 coincides with the usual definition of the gas parameter na_s^3 in the limit of vanishing dipolar interaction, that is $C_{dd} \to 0$. See also below and Refs. [29, 30].
[28] T. Lahaye, C. Menotti, L. Santos, M. Lewenstein, and T. Pfau, Reports on Progress in Physics **72**, 126401 (2009).
[29] D. C. E. Bortolotti, S. Ronen, J. L. Bohn, and D. Blume, Phys. Rev. Lett. **97**, 160402 (2006).
[30] S. Ronen, D. C. E. Bortolotti, D. Blume, and J. L. Bohn, Phys. Rev. A **74**, 033611 (2006).
[31] M. A. Baranov, M. Dalmonte, G. Pupillo, and P. Zoller, Chemical Reviews **112**, 5012 (2012).
[32] B. Svistunov, E. Babaev, and N. Prokof'ev, *Superfluid States of Matter* (Taylor & Francis, 2015).
[33] E. L. Pollock and D. M. Ceperley, Phys. Rev. B **36**, 8343 (1987).
[34] D. M. Ceperley, Rev. Mod. Phys. **67**, 279 (1995).
[35] P. Jain, F. Cinti, and M. Boninsegni, Phys. Rev. B **84**, 014534 (2011).
[36] An extensive calculation of the critical temperature in the presence of dipolar interactions is not reported here. Indeed it can be done along the lines of the analysis of [39] and it is the focus of an ongoing separated investigation.
[37] M. A. Baranov, Physics Reports **464**, 71 (2008).
[38] A. R. P. Lima and A. Pelster, Phys. Rev. A **84**, 041604 (2011).
[39] S. Pilati, S. Giorgini, and N. Prokof'ev, Phys. Rev. Lett. **100**, 140405 (2008).